doi.org/10.36721/PJPS.2026.39.7.188.1

Isolation of banana lectin from *Musa paradisiaca* and investigation of its interactions with selected anticancer drugs: Insights from spectroscopic, computational and cellular studies

Rida Arif[1], Javeria Arif[2], Zoha Warsi[3], Syeda Sarah Tahir[3] and Saima Rasheed[3]*

[1]H. E. J. Research Institute of Chemistry, International Center for Chemical and Biological Sciences, University of Karachi, Karachi-75270, Pakistan

[2]Department of Pharmacy, Sardar Bahadur Khan Women's University, Quetta, Pakistan

[3]Dr. Panjwani Center for Molecular Medicine and Drug Research, International Center for Chemical and Biological Sciences, University of Karachi, Karachi-75270, Pakistan

Abstract: **Background**: Banana lectin (Banlec), a mannose/glucose-specific lectin isolated from *Musa paradisiaca*, is known for its immunomodulatory, antiviral and anticancer properties. However, its molecular interactions with anticancer drugs remain insufficiently explored, limiting its translational potential in targeted drug delivery. **Objectives**: This study aimed to purify Banlec and systematically investigate its binding interactions with selected FDA-approved anticancer drugs, dasatinib, 5-fluorouracil (5-FU) and anastrozole, to gain mechanistic insights into Banlec-drug recognition and stability. **Methods**: Banlec was purified from ripened *Musa paradisiaca* fruit using affinity chromatography. Binding interactions were examined using UV-Visible spectroscopy, circular dichroism (CD), differential scanning fluorimetry (DSF) and hemagglutination inhibition assay. Docking and molecular dynamics simulations were performed to analyze binding modes and complex stability. Additionally, the anticancer activity of Banlec and its drug-bound complexes was assessed against HL-60 cells using the MTT assay. **Results**: Banlec was purified from ripened *Musa paradisiaca* and characterized as a homodimeric protein (~30 kDa). UV–Visible spectroscopy confirmed spontaneous Banlec-drug interactions. CD analysis showed that Banlec retained its secondary structure upon binding with dasatinib and 5-FU, whereas pronounced conformational changes were observed with anastrozole. DSF analysis showed slight thermal stabilization with dasatinib and 5-FU, while anastrozole caused thermal destabilization. Hemagglutination inhibition assays indicated that the selected drugs did not mask the Banlec carbohydrate-binding domains and therefore its glycan-targeting potential is retained. Docking and MD simulations showed strongest binding with dasatinib, providing maximal stabilization, followed by 5-FU with moderate stabilization. Notably, among the evaluated complexes, Banlec–5-FU complex exhibited the most potent anticancer activity against HL-60 cells, compared to Banlec and 5-FU alone. **Conclusion**: This study provides the first comprehensive insight into Banlec–anticancer drug interactions, identifying 5-FU as the most favorable binding partner. The findings highlight Banlec as a promising scaffold for development of glycan-targeted anticancer drug delivery systems and expand its therapeutic potential.

Keywords: Banana lectin (Banlec); Circular dichroism spectroscopy; DSF analyses; 5-Fluorouracil (5-FU); Human promyelocytic leukemia (HL-60) cells; Molecular dynamics simulation

Submitted on 21-12-2025 – Revised on 05-03-2026 – Accepted on 16-03-2026

INTRODUCTION

Lectins are a structurally diverse group of non-immune carbohydrate-binding proteins that mediate a broad range of biological processes, including cell–cell communication, immune modulation and host–pathogen recognition (Naithani *et al.,* 2021; Neetu *et al.,* 2025). Among plant lectins, Banana lectin (Banlec) has received considerable attention due to its diverse biological activities, such as antiviral, immunopotentiating and anticancer activities (De Camargo *et al*., 2020; Cheung *et al.,* 2009; Boliukh *et al.,* 2024). Banlec belongs to the jacalin-related lectin (JRL) family and exhibits a high affinity for mannose-containing glycans, enabling it to recognize glycoproteins and glycolipids on the cell surface (Singh *et al*., 2014; Koshte *et al*., 1990). Banlec has been isolated from three different *Musa* species; Koshte and coworkers reported the isolation of Banlec from *Musa paradisiaca*, Peumans *et al.,* reported from *Musa acuminata*, while Wong and Ng reported its isolation from *Musa basjoo* (Koshte *et al*., 1990; Peumans *et al*., 2000; Wong and Ng, 2006).

Musa paradisiaca is a commonly cultivated banana species in Pakistan. Following the first isolation of Banlec from *Musa paradisiaca* by Koshte and coworkers, it has been extensively studied for its structural, functional and biological properties, underscoring its significance in lectin research. Early studies by Singh *et al.,* achieved the first crystallization and preliminary X-ray structure analysis of Banlec, laying the groundwork for structural investigations (Singh *et al*., 2004). Building on this, Singh *et al.,*

**Corresponding author:* e-mail: saimarasheed1@hotmail.com

demonstrated Banlec's unusual sugar-binding specificity and suggested its evolutionary relationship with other monocot lectins (Singh *et al*., 2005). Meagher *et al.,* further discovered a novel second sugar-binding site in Banlec, providing key insights into its carbohydrate recognition mechanisms (Meagher *et al.,* 2005). Subsequent biophysical work by Gupta *et al*., explored Banlec's unfolding energetics and stability, highlighting its structural robustness (Gupta *et al*., 2008). Liu and coworkers, further expanded its functional studies and biological relevance and reported that Banlec binds to the tobacco mosaic virus capsid protein, inhibiting viral infection (Liu *et al*., 2014). Research group of Batcha demonstrated its *in vitro* antiviral activity against herpes simplex viruses (HSV-1 and HSV-2) (Batcha *et al*., 2020). Degroote and colleagues reported that Banlec is mitogenic for cow and pig PBMCs *via* the IL-2/ELF1 pathway (Degroote *et al*., 2021) while Mahaboob Batcha and coworkers revealed that purified Banlec induces apoptosis in cancer cell lines, emphasizing its therapeutic potential (Mahaboob Batcha *et al*., 2023). Together, these studies highlight Banlec as a structurally unique and biologically versatile lectin with diverse biological applications.

Beyond its intrinsic bioactivities, Banlec's strong and selective affinity for specific glycan residues on cell surfaces makes it a promising candidate for targeted drug delivery, particularly in conjugation with anticancer drugs. Lectin-mediated targeting takes advantage of the distinct glycosylation patterns that distinguish healthy from malignant cells, enabling site-specific drug delivery and improved therapeutic efficacy. The structural stability and dual carbohydrate-binding sites of Banlec could be employed to develop lectin–drug conjugates capable of improving the specificity of anticancer therapy while minimizing off target toxicity. Despite Banlec's potential for targeted drug delivery, no studies have yet reported describing its direct binding or conjugation with anticancer drugs. In contrast, the use of various plant lectins, including wheat germ agglutinin and the galactose-binding lectin from *Vatairea macrocarpa* seeds, for the binding and delivery of anticancer and antimicrobial agents has been well documented, demonstrating the feasibility of lectin-mediated drug targeting (Zhou *et al*., 2015; Yin *et al*., 2006; Lavelle *et al*., 2004; Santos *et al*., 2020). Therefore, investigating Banlec–drug interactions offer a promising and largely unexplored avenue for the development of targeted anticancer therapies.

The objective of the present study was to isolate the Banlec from *Musa paradisiaca* and to study its binding interactions with three most widely used anticancer drugs, 5-fluorouracil, dasatinib and anastrozole, using a combination of spectroscopic and computational techniques, supported by cellular evaluation against the HL-60 leukemia cells. Insights into the molecular interactions between Banlec and these drugs may contribute to a better understanding of their binding behavior and could serve as a preliminary step toward exploring glycan-targeted approaches for anticancer applications. Since no prior studies have been reported describing the binding interactions of aforementioned anticancer drugs with Banlec, the present work aims to fill this knowledge gap and advances the understanding of Banlec's potential role in targeted drug delivery.

MATERIALS AND METHODS

Anticancer drugs i.e., 5-fluorouracil, dasatinib and anastrozole were obtained from the Molecular Bank, Dr. Panjwani Center for Molecular Medicine and Drug Research (PCMD), International Center for Chemical and Biological Sciences (ICCBS), University of Karachi, Pakistan. Banana lectin (Banlec) was isolated and purified from ripe bananas purchased from the local fruit market of Karachi, Pakistan. The banana species (*Musa paradisiaca*, G.H. No. 96034) was identified by the Center for Plant Conservation, Karachi University Herbarium and Botanic Garden, University of Karachi. All other chemicals utilized in this study were of high purity and analytical grade.

Purification of banana lectin from banana fruit

Banlec was isolated following the procedure described by Kumar and Surolia with slight modifications (Gnanesh Kumar and Surolia, 2018). In brief, 160 g ripe bananas were soaked in 200 mL of 10 mM phosphate-buffered saline; PBS (pH 7.4; containing 2% (v/v) acetic acid) and incubated for 3 days at 4 °C. After incubation, the mixture was filtered through muslin cloth to remove debris. The filtrate was centrifuged at 7000 rpm for 20 min at 4 °C and the resulting gelatinous pellet was discarded. The supernatant was then saturated with 65% ammonium sulfate and gently stirred overnight at 4 °C. Following protein precipitation, the mixture was centrifuged at 10,000 rpm for 30 min at 4 °C. The supernatant was discarded and the pellet was resuspended in PBS (10 mM, pH 7.4) and dialyzed against the same buffer for 48 h to remove residual salts. Purification of Banlec was performed using a Superdex™ 75 column (Cytiva), conventionally used for size-exclusion chromatography; its matrix consists of cross-linked dextran and agarose polysaccharides that present abundant carbohydrate moieties capable of interacting with lectins. Owing to the intrinsic mannose/ glucose binding specificity of Banlec, the lectin exhibited selective affinity toward the carbohydrate-rich matrix, resulting in retention on the column through carbohydrate–protein interactions. The column was pre-equilibrated with PBS (10 mM, pH 7.4) and the filtered protein solution was loaded onto it. Unbound proteins were eluted using the same buffer, while bound Banlec was eluted with methyl-*α*-D-glucopyranoside (400 mM). The purity of eluted fractions was analyzed by 15% SDS–PAGE and those showing a single band were pooled and dialyzed against double-distilled water for 36 h and subsequently

concentrated using Amicon® Ultra-15 centrifugal filters (10 kDa MWCO) for further studies.

Spectroscopic analyses of Banlec–drugs interactions

UV-Visible spectroscopic analyses

UV-Visible spectra were recorded using a Shimadzu UV-1800 UV-Visible spectrophotometer (Kyoto, Japan) with 1 cm quartz cuvette at room temperature. For the interaction studies, a constant concentration of Banlec (25 µM) was mixed with different concentrations of anticancer drugs, such as 1000 to 3.9 µM concentrations (2-fold dilutions) of dasatinib and anastrozole was used, while 125 to 0.97 µM concentrations (2-fold dilutions) of 5-FU were used. Banlec and aforementioned drugs were incubated for 15 minutes at 4 °C. After incubation, full scan UV-Visible measurements (from 190 to 800 nm) were recorded for comparative analysis of interactions, while binding titrations were monitored specifically at 280 nm to detect drug-induced variations in the UV absorbance spectrum of Banlec (Munir *et al*., 2017). The experiments were performed in triplicates to ensure reproducibility and data is presented as mean ± standard deviation (SD). The binding constants (K_b) of Banlec with the selected anticancer drugs were calculated using the Benesi–Hildebrand equation (1),

$$1/\Delta A = 1/(\Delta\varepsilon\,[\text{Banlec}]\,k_b) \times 1/([\text{ligand}]) \quad (1)$$

Where; Δε is change in absorption coefficient; ΔA is change in absorbance of protein before and after the addition of ligand; [Banlec] is the concentration of Banlec and [ligand] is the concentration of anticancer drug, i.e., anastrozole, dasatinib and 5-FU. Gibb's free energy ΔG^o of the interaction of Banlec and anticancer drugs were calculated using equation 2:

$$\Delta G^\circ = -RT \ln K_b \quad (2)$$

Where; R= ideal gas constant (J mol^{-1} K^{-1}); and T= temperature (in K).

CD spectroscopic analyses

The secondary structure and conformational characteristics of Banlec, both in its native state and in complex with anticancer drugs, were analyzed using circular dichroism (CD) spectroscopy. Banlec and anticancer drugs were used at 3 and 1000 µM concentrations, respectively. CD spectra for the corresponding samples were recorded using a Spectro-polarimeter (Jasco J810, Japan) at a resolution of 0.5 nm, utilizing a 2 mm path length sample cell. An average of four complete wavelength scans was performed in the far-UV amide region (190–250 nm) at 25 °C (Munir *et al*., 2017; Nazir *et al*., 2024). The solvent subtracted spectra were converted to mean residue ellipticity (MRE) using equation 3:

$$\text{MRE} = \text{Observed CD (mdeg)}/ (10\, C_p\, n\, l) \quad (3)$$

Where Cp denotes the molar concentration of Banlec, n represents the number of amino acid residues (282 amino acid residues are found in Banlec) and l indicates the path length of the quartz cell. The CD spectra were analyzed further for secondary structure estimation (SSE) using the BeStSel web server (Micsonai *et al*., 2015).

Differential scanning fluorimetry (DSF)

The fluorescence-based assay was employed to investigate the effect of anticancer drugs on the thermal stability of Banlec. The melting temperature of purified Banlec, both in its native form and in complex with anticancer drugs, was evaluated using a real-time PCR machine (Bio-Rad Laboratories, USA), following the procedures described by Kumar and Surolia (Gnanesh Kumar and Surolia, 2018). The total reaction volume was 25 µL in each PCR tube (containing Banlec (10 µM), anticancer drugs (1 mM) and Sypro® Orange dye (2x)). The reaction mixtures were then subjected to a temperature ramp from 20 to 95 °C at a rate of 0.3 °C/min. Fluorescence intensity was recorded using the Hex channel (Ex/Em: 538/555 nm) to monitor temperature-dependent changes in fluorescence intensity. Data were analyzed using CFX Manager™ software (Bio-Rad Laboratories, USA). All experiments were performed in triplicate and data are reported as the mean ± standard deviation (SD).

Hemagglutination inhibition assay (HI)

The hemagglutination inhibition assay was performed in a 96-well microtitre plate using 2% human RBCs suspension. The experimental protocol was approved by the "Independent Ethics Committee (IEC)" of the ICCBS, University of Karachi under Study #ICCBS/IEC-098-HB/2023 and written informed consent was taken from participants prior to sample collection. Six healthy adult volunteers, aged 20–28 years, with no known hematological disorders, were recruited for the study. Human blood (O^+) was taken in sodium citrate vacutainer. Fresh human RBCs were separated from plasma by centrifugation at 3500 × g for 5 minutes at 4 °C. The plasma and buffy coat were carefully removed. After 3 washes with 10 mM phosphate-buffered saline (PBS), the erythrocytes were diluted to 2% concentration with PBS containing 0.005% sodium azide. For the inhibition assay, Banlec (1000 µg/mL; 20 µL) was pre-incubated with three different concentrations (i.e., 100, 50 and 25 mM) of selected ligands (i.e., anastrozole, dasatinib and 5-FU) for 15 minutes at room temperature. Subsequently, 20 µL of 2%, human RBCs suspension was added to each well. The plate was incubated at room temperature for 1 hour and results were visually analyzed (Adamova *et al.,* 2014).

In-silico studies

The 3D configurations of selected anticancer drugs were retrieved from the PubChem database and subjected to energy minimization *via* ChemBioDraw Ultra 12.0 (CambridgeSoft). The crystal structure of the native Banana lectin (PDB ID: 2BMY) was acquired from the Protein Data Bank (www.rcsb.org). Molecular docking

studies were executed using AutoDock 4.2, utilizing the Lamarckian Genetic Algorithm (LGA) for conformational sampling. Protein preparation involved adding polar hydrogens, merging non-polar hydrogens and assigning Kollman charges using AutoDock Tools (Morris *et al*., 2008). Blind docking was carried out with a grid box that covered the entire surface of the protein. The protein remained rigid, while the ligands were allowed full torsional flexibility. Visualization and interpretation of docking results were performed using CCP4mg (McNicholas *et al*., 2011).

Molecular dynamics simulation

Molecular dynamics (MD) simulations were carried out at an atomic level to evaluate the structural changes and interaction stability of protein-ligand complexes employing the GROMACS software package (Abraham *et al.,* 2015). MD simulations offer significant insight into biomolecular systems' structural flexibility, stability and binding behavior, allowing for the rational development of new therapeutic techniques (Chitongo *et al.,* 2020). In the present study, considering the molecular docking results, simulations of the *apo* Banlec and its three drug complexes (i.e., Banlec-Dasatinib (C1) complex, Banlec-5-Fluorouracil (C2) complex and Banlec-Anastrozole (C3) complex) were performed. In each system, the protein topology was built using the AMBER99SB force field (Hornak *et al.,* 2006), while the ligand topology generated *via* ACPYPE (Sousa da Silva and Vranken, 2012). The systems were solvated utilizing the Tip3 water model in a cubic periodic boundary box and neutralized with Na^+ and Cl^- ions under physiological conditions (Jorgensen *et al.,* 1983). Energy minimization of all the system were performed with the steepest descent algorithm for 5000 steps to remove unfavorable clashes, followed by equilibration at 300 K and 1 bar pressure using NVT and NPT conditions, with a thermostat relaxation time of 1000 ps (Martoňák *et al.,* 2003; Martyna *et al.,* 1992). Finally, 100 ns production runs were conducted on all systems and the resulting trajectories were assessed to reveal structural and dynamic properties such as root mean square deviation (RMSD), root mean square fluctuation (RMSF) and radius of gyration (Rg).

Anticancer activity against human leukemic HL-60 cells

Anticancer activity of Banlec alone and its drug-bound complexes was evaluated against HL-60 cells using MTT cell proliferation assay, which is widely used to assess cell viability and proliferation, as well as the cytotoxic or cytostatic effects of drug leads. The experiments were performed on HL-60 cells (human promyelocytic leukemia cell line; CLS-300209) obtained from Bio Bank Facility, PCMD, ICCBS. The cells were cultured in RPMI-1640 media supplemented with 10% FBS (fetal bovine serum) and 1% antibiotics (10,000 µg/mL streptomycin and 10,000 unit /mL penicillin) at 37 °C in a humidified atmosphere with 5% CO_2, under standard conditions. The media was changed twice a week. All experimental procedures were carried out in the log-phase of cell growth. In order to perform MTT assay, 8×10^4 HL-60 cells were seeded on 96-well plates and incubated for 24 hours at 37 °C in a humidified atmosphere with 5% CO_2. Banlec was dissolved in 10 mM PBS, while test compounds were dissolved in DMSO (0.1% final concentration) or water. The control wells contained either PBS or water or DMSO. The HL-60 cells were incubated with test compounds for 48 hours. After incubation, 20 µL of MTT (3-(4,5-dimethylthiazol-2-yl)-2,5-diphenyltetrazolium bromide) solution (0.5 mg/mL) was added to each well and plates were further incubated for 4 hours yielding purple MTT formazan crystals in the wells. In the next step, 96-well plates were centrifuged for 5 min at 1200 rpm and the supernatant was discarded. The formazan crystals were dissolved by adding 100 µL of DMSO in each well of 96-well plate and kept in dark for 5 min. Finally, the change in absorbance was recorded at 550 nm using a microplate reader. Doxorubicin was used as the standard anticancer drug (IC_{50} = 0.000098 ± 0.000003 mg/mL) (Rahman *et al.,* 2024). Results were expressed as mean ± standard error of mean (SEM) from triplicate experiments, % inhibition was calculated using equation 4, while IC_{50} values were calculated using the EZ-Fit Enzyme Kinetic program.

$$\% \text{ Inhibition} = 100 - \left[\frac{(\text{Absorbance of test compound} - \text{Absorbance of negetive control})}{(\text{Absorbance of positive control} - \text{Absorbance of negetive control})} \text{ x } 100\right] \quad (4)$$

RESULTS

Purification and characterization of banana lectin (Banlec)

Banlec was isolated from ripened fruit of *Musa paradisiaca* (banana) as a homodimeric protein with a molecular weight of ~30 kDa. SDS-PAGE analysis under reducing conditions revealed a distinct band at approximately 15 kDa, corresponding to the monomeric subunit of Banlec (Fig. 1). The identification of the purified protein was inferred based on its expected molecular weight and lectin-specific elution behavior during purification, in agreement with earlier reports on banana lectin purification (Koshte *et al.,* 1990; Peumans *et al.,* 2000).

Spectroscopic analyses to study the binding interactions between Banlec and anticancer drugs

UV-Visible spectroscopic analyses

The binding interactions between Banlec and selected anticancer drugs (i.e., anastrozole, dasatinib and 5-FU) were analyzed using UV-Visible spectroscopy. Initial baseline absorbance spectra were recorded across the wavelength range of 190–800 nm using a reference cuvette containing only the solvent (water for water-soluble ligands, or ≤1% v/v DMSO for water-insoluble ligands). All UV–visible spectra were baseline-corrected against the corresponding solvent blank. Results revealed that native Banlec showed the absorption maxima at 280 nm,

characteristic of proteins due to their aromatic amino acids (i.e., tryptophan, tyrosine and phenylalanine). However, none of the selected ligands displayed distinct absorbance, except for 5-FU, which exhibited absorption maxima at 266 nm (Fig. 2). Consequently, for the Banlec–5-FU complex, the absorbance spectra of free 5-FU at corresponding concentrations were recorded under identical experimental conditions and subtracted from the protein–ligand spectra to ensure that the observed spectral changes were attributable solely to ligand-induced perturbations in the protein environment.

It is well reported that Banlec is a mannose binding protein (Swanson *et al.*, 2010); therefore, preliminary titration studies were performed using mannose as the reference ligand. UV–Visible absorption spectra of native Banlec (25 µM) in the presence of increasing concentrations of D-mannose (1000 to 3.9 µM; two-fold serial dilutions) is shown in figure 2A. Results revealed that the characteristic absorbance peak at 280 nm, decreases progressively with increased mannose concentration (i.e., hypochromic effect), indicating binding-induced changes in the protein environment. The inset of Fig. 2A displays the Benesi–Hildebrand plot (1/A *vs* 1/[D-mannose]), used to determine the binding constant (K_b), which was calculated to be (1.28 ± 0.01) × 10^5 M^{-1} with a strong linear correlation (R^2 = 0.9869), confirming a high-affinity interaction between Banlec and D-mannose.

In the next step, the UV–visible absorption spectra of Banlec were recorded in the absence and presence of increasing concentrations of selected anticancer drugs. Addition of anastrozole caused a hypochromic effect (decrease in absorbance at 280 nm). Dasatinib induced both a hypochromic effect and a slight hypsochromic shift (i.e., λ_{max} changed from 280 nm to 277 nm), whereas addition of 5-FU also induced a hypochromic effect accompanied by a more pronounced blue shift from 280 to 266 nm. These spectral changes suggest that these drugs stabilize the protein structure, possibly *via* hydrogen bonding or hydrophobic interactions, which reduce the solvent exposure of aromatic residues, resulting in the observed hypochromic effect. The observed blue shift may result from a decrease in polarity or an increase in hydrophobicity around the chromophoric residues upon ligand binding. Overall, these findings indicate complex formation between Banlec and the drugs, reflecting ligand-induced modifications in the microenvironment of aromatic residues (Azeem *et al.,* 2024; Adamczyk *et al.,* 2023; Abdi *et al.,* 2012) (Fig. 2; Table 1).

Benesi–Hildebrand plots were also generated for all Banlec–drug complexes to evaluate the strength of binding interactions (Fig. 2). The observed linearity in each plot validated the formation of stable complex between Banlec and selected anticancer drugs. The Banlec-dasatinib exhibited the highest binding affinity (K_b = (1.65 ± 0.09) ×10^5 M^{-1}), slightly greater than that of the reference Banlec-mannose complex (K_b = (1.28 ± 0.01) × 10^5 M^{-1}) followed by the Banlec-5-FU complex (K_b = (1.41 ± 0.03) ×10^5 M^{-1}), whereas the Banlec-anastrozole complex displayed the weakest interaction (K_b = (5.1± 0.03) ×10^2 M^{-1}). The negative Gibbs free energy (ΔG°) values further indicated that these interactions are spontaneous and thermodynamically feasible (Table 1).

CD spectroscopic analyses

Far-UV CD spectra were obtained for Banlec both in native state and in complex with each drug to analyze any conformational changes induced by the drugs. The native Banlec exhibited a negative trough between 210 and 230 nm, a typical feature of lectins with a β-sheet-rich secondary structure, which aligns well with the findings previously reported by Khan *et al.* (Khan et *al*., 2013). Quantitative spectral analysis for secondary structure estimation (SSE) also revealed that native Banlec predominantly possess a β-sheet secondary conformation, characterized by 29.9% antiparallel and 34.3% parallel β-sheet content (Fig. 3). Results revealed that complexation with dasatinib and 5-fluorouracil (5-FU) induced a slight decrease in the ellipticity of Banlec's CD spectra, suggesting minor alterations in its secondary structure, while the position of the characteristic broad negative band between 210-230 nm remained unchanged, suggesting these drugs did not affect the β-sheet conformation of Banlec. Secondary structure deconvolution revealed minor conformational changes in antiparallel and parallel β-sheets upon binding with dasatinib and 5-FU, without disturbing the overall β-sheet-rich architecture of Banlec. In case of Banlec- dasatinib complex antiparallel β-sheets were slightly reduced from 29.9% to 23.5%; while parallel β-sheets from 34.3% to 31.5%. In case of Banlec-5-FU complex the antiparallel β-sheets slightly reduced from 29.9% to 22.8%, while parallel β-sheets reduced from 34.3% 32.2% (Fig. 3B). In contrast, the Banlec-anastrozole complex showed substantial changes in the ellipticity of Banlec's CD spectra. The characteristic spectral profile was disrupted, with a pronounced decrease in peak intensity and loss of the β-sheet content, indicative of significant structural destabilization of Banlec (Fig. 3). All these changes suggested that Banlec preserved its secondary structure upon interaction with dasatinib and 5-FU.

Effect of selected anticancer drugs on thermal stability of Banlec

The melting temperature (Tm) of native Banlec was found to be 71.40 ± 0.17 °C, which is consistent with the previously reported data (Gnanesh Kumar and Surolia, 2018). Upon binding with the selected anticancer drugs (i.e., dasatinib, 5-FU and anastrozole) distinct effects on Banlec's thermal stability were observed. The Banlec-dasatinib and Banlec-5-FU complexes exhibited increased Tm values of 72.2 ± 0.30 °C (ΔTm = +0.8 °C) and 72.8 ±

0.30°C (ΔTm = +1.4°C), respectively, indicating a stabilizing effect on the protein structure. In contrast, the Banlec-anastrozole complex showed a reduced Tm of 69.7 ± 0.17°C (ΔTm = -1.7°C), suggesting a destabilizing effect on Banlec (Fig. 4).

Hemagglutination inhibition assay (HI)

Hemagglutination inhibition assay was performed to determine whether binding of the selected drugs interferes with the carbohydrate-binding domains of banana lectin, which are essential for erythrocyte recognition and targeting. Banlec has been previously reported to exhibit hemagglutinating activity (De Camargo *et al.,* 2020) and consistent with this property, the assay was first conducted using D-mannose as a reference inhibitor. D-mannose completely inhibited the Banlec induced hemagglutination at 50 mM, 25 mM and 12.5 mM concentration, evidenced by the presence of a distinct red dot at the bottom of the well (Fig. 5A). While selected anticancer drugs (i.e., anastrozole, dasatinib and 5-FU) did not inhibit the Banlec induced hemagglutination at any tested concentration (Fig. 5B-D).

Molecular docking

Molecular docking is used to predict drug–protein interactions and binding modes mediated by noncovalent forces. Herein, molecular docking studies were performed as a supportive, exploratory tool to predict potential binding interactions and estimate the binding affinities of the selected anticancer drugs (i.e., anastrozole, dasatinib and 5-FU) with Banlec, complementing the experimental binding analyses. The overall structural organization of Banlec, including its carbohydrate-binding sites and secondary binding regions, is illustrated in Scheme-1.

The binding affinity of anastrozole was found to be -4.69 kcal/mol. Analysis of the docking pose revealed a single hydrogen bond between the N4 atom of anastrozole and the backbone oxygen of Pro22 at a distance of 3.2 Å, highlighting Pro22 as the principal residue mediating anastrozole recognition within the Banlec structure (Fig. 6).

Dasatinib showed the most favorable predicted binding affinity (-6.52 kcal/mol), consistent with the trend observed in UV–Visible binding studies, suggesting a comparatively stronger interaction. The docking pose indicated that dasatinib is positioned within the Greek key III region of Banlec, where it participated in stabilizing hydrogen-bonding interactions with Gly105 and Asn106 amino acid residues (Fig. 7). Specifically, nitrogen atom (N8) of dasatinib participated in a hydrogen-bond interaction with a backbone heteroatom (N) of Gly105, at a bond distance of 3.0 Å. Similarly, the N7 atom of dasatinib formed a hydrogen bond with the side-chain ND2 atom of Asn106 at a bond distance of 2.9 Å, indicative of stabilizing polar contacts.

The predicted binding affinity for 5-FU was –5.23 kcal/mol, which was lower than that observed for dasatinib. Relative to dasatinib, the docked pose of 5-fluorouracil (5-FU) indicated potential hydrogen-bonding interactions with Pro103, Asn106 and His63 amino acid residues of Banlec (Fig. 8). Nitrogen atom (N5) of 5-FU participated in a hydrogen-bond interaction with a backbone oxygen atom of Pro103 at a bond distance of 3.1 Å. In addition, the N4 and O2 atoms of 5-FU showed hydrogen-bonding interactions with the side-chain OD1 and ND2 atoms of Asn106, with bond distances of 2.7 Å and 3.1 Å, respectively. Furthermore, the F1 atom of 5-FU showed a hydrogen bond interaction with the NE2 atom of His63 at a bond distance of 3.0 Å, contributing to the stabilization of the docked complex (Fig. 8).

Molecular dynamics simulation

Initially, molecular docking studies provided the binding poses and identified key interacting residues in the Banlec–drug complexes. To account for protein flexibility and understand the dynamics behavior relatively close to the physiological condition, these complexes were subjected to 100 ns molecular dynamics simulations. Molecular dynamics simulations are highly useful for gaining thorough insights into complex biological systems and their periodic dynamics (Zhu *et al.,* 2025). These simulations further validated the docking results and allowed analysis of ligand-dependent conformational changes in both the *apo* protein and ligand-bound complexes.

The structural stability of the Banlec protein in its *apo* form and in complex with three drugs; dasatinib (C1), 5-FU (2) and anastrozole (C3) was examined by calculating RMSD over a 100 ns molecular dynamics simulation, as shown in Fig. 9. The *apo* protein exhibited an initial equilibration phase followed by a slight increase and stabilization around 0.20 to 0.25 nm RMSD value, showing moderate conformational adjustments during the simulation. In comparison, the Banlec–dasatinib (C1) complex revealed relatively small RMSD values, stabilizing the backbone between 0.14-0.18 nm RMSD values across the trajectory, pointing to enhanced structural stability and lower backbone deviations upon ligand binding. The Banlec-5-FU (C2) complex behaved similarly to the *apo* form, stabilizing at 0.18-0.21 nm after initial fluctuations, indicating a stable association with minor conformational changes. In contrast, the Banlec-anastrozole (C3) complex exhibited comparatively greater RMSD values, with noticeable fluctuations measured notably after 70 ns, indicating increased flexibility and wider structural changes upon ligand binding.

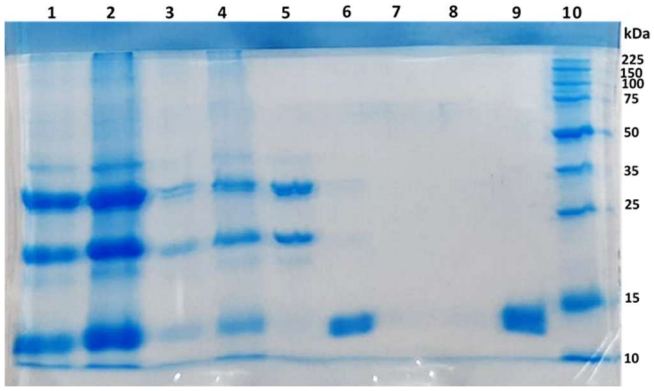

Fig. 1: SDS-PAGE analysis of purified Banlec. Lane 1-4: crude extract of bananas; lane 5: unbound protein after affinity chromatography; lane 6: Banlec eluted after affinity chromatography; lane 9: concentrated Banlec; lane 10: protein marker.

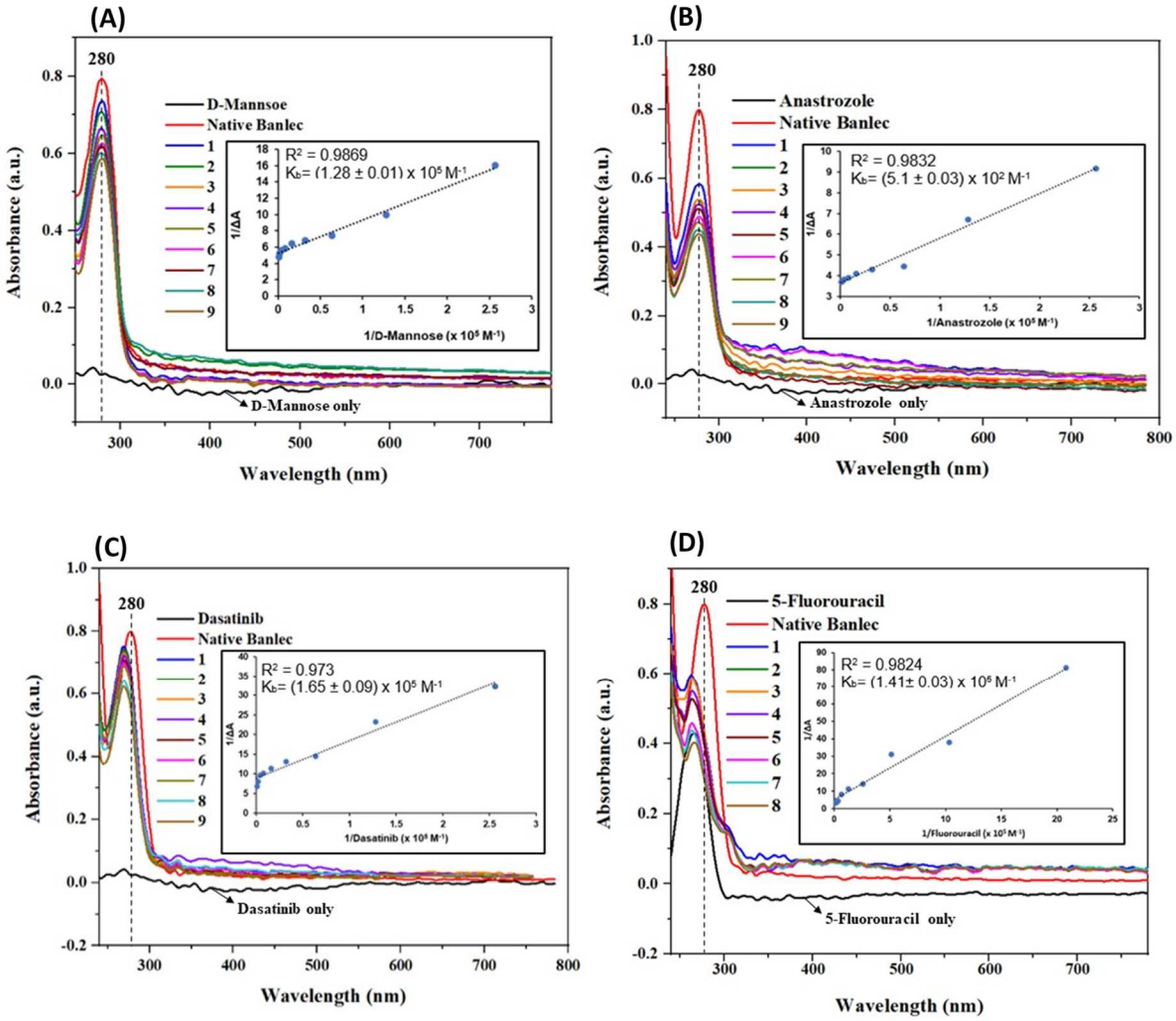

Fig. 2: UV–Visible spectroscopic analyses of Banlec in its native state and in the presence of varying concentrations of D-mannose and selected anticancer drugs, along with the corresponding Benesi–Hildebrand plots. (A) Banlec–mannose complex, (B) Banlec–anastrozole complex, (C) Banlec–dasatinib complex, and (D) Banlec–5-fluorouracil (5-FU) complex. For D-mannose, anastrozole, and dasatinib, concentrations ranged from 3.9 to 1000 µM (two-fold serial dilutions labeled 1–9), whereas for 5-FU, concentrations ranged from 0.97 to 125 µM (two-fold serial dilutions labeled 1–8).

Table 1: Binding constant and Gibbs free energy for Banlec complexes.

S. No.	Complex	Binding constant (K_b) (M^{-1})	Gibbs free energy (ΔG^o) (kJ mol^{-1})
1.	Banlec- Mannose	$(1.28 \pm 0.01) \times 10^5$	-28.7
2.	Banlec- Anastrozole	$(5.1 \pm 0.03) \times 10^2$	-15.5
3.	Banlec- Dasatinib	$(1.65 \pm 0.09) \times 10^5$	-29.7
4.	Banlec- Fluorouracil	$(1.41 \pm 0.03) \times 10^5$	-29.3

(A)

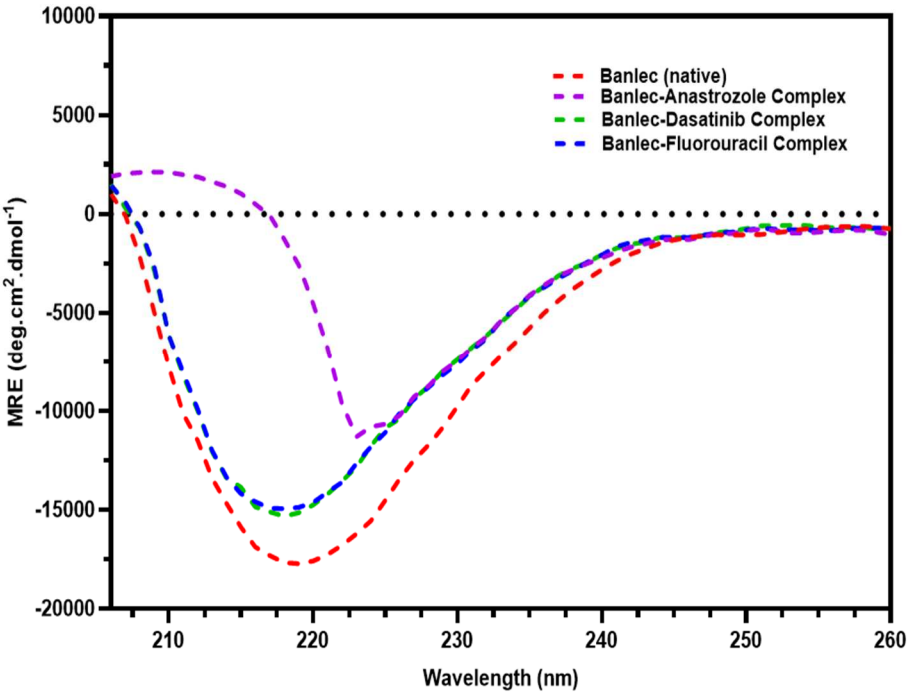

(B)

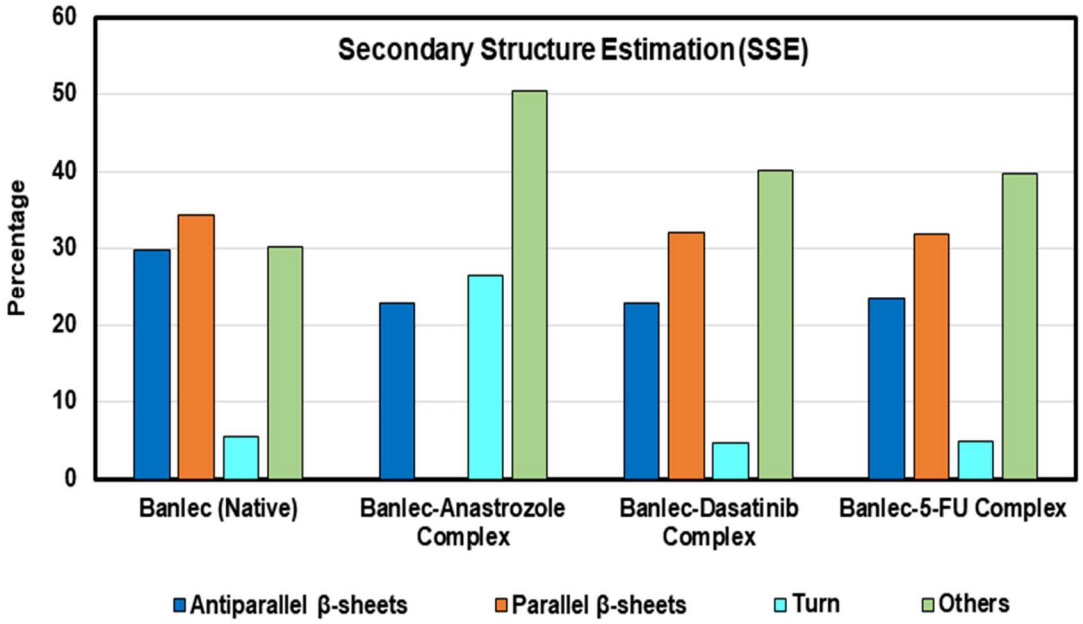

Fig. 3: Circular dichroism (CD) spectroscopic analyses. (A) CD spectra of Banlec (native form), and in complex with different anticancer drugs; (B) Secondary structure estimation (SSE).

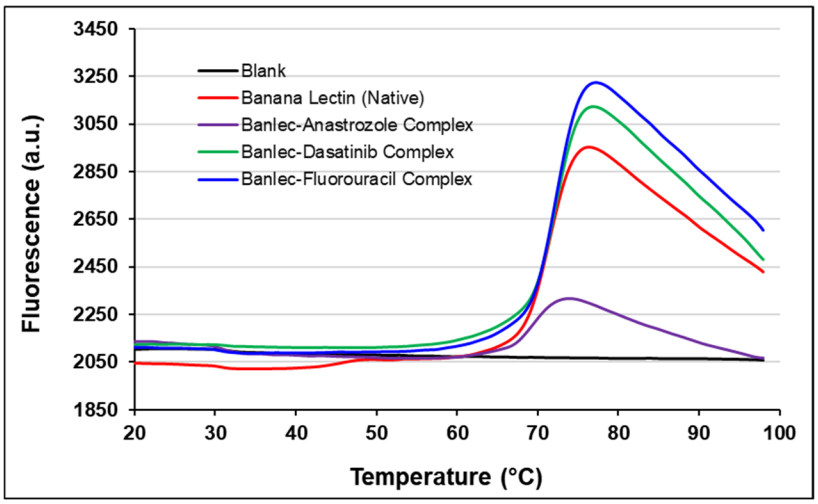

Fig. 4: Thermal denaturation profile of Banlec in native form, and in complex with different anticancer drugs.

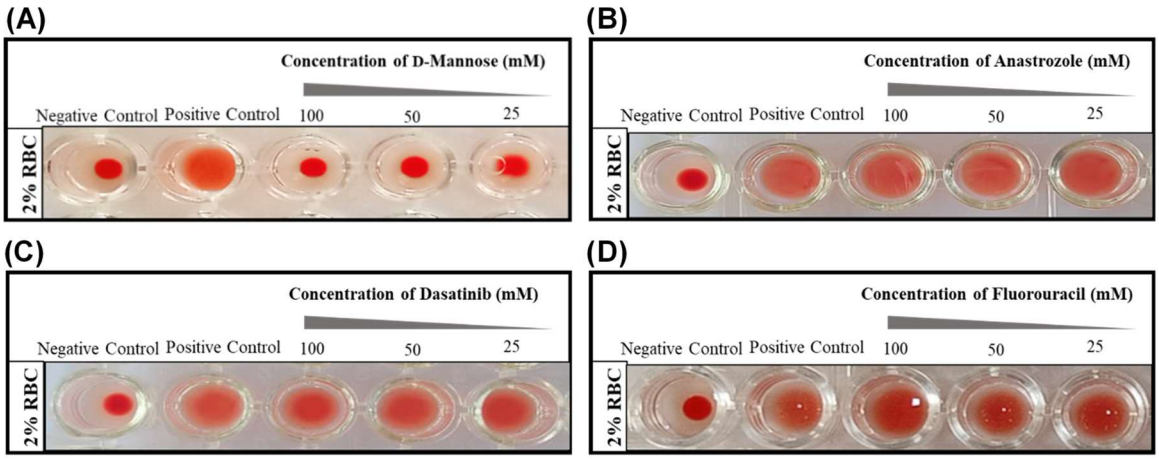

Fig. 5: Banlec-induced hemagglutination inhibition of (2%) RBCs by D-mannose and selected anticancer drugs (100 - 25 mM; two-fold dilutions). (A) D-Mannose, (B) Anastrozole, (C) Dasatinib, (D) Fluorouracil. Negative control wells contained 2% RBCs in PBS, while the positive control contained Banlec (1000 µg/mL) with 2% RBCs in PBS.

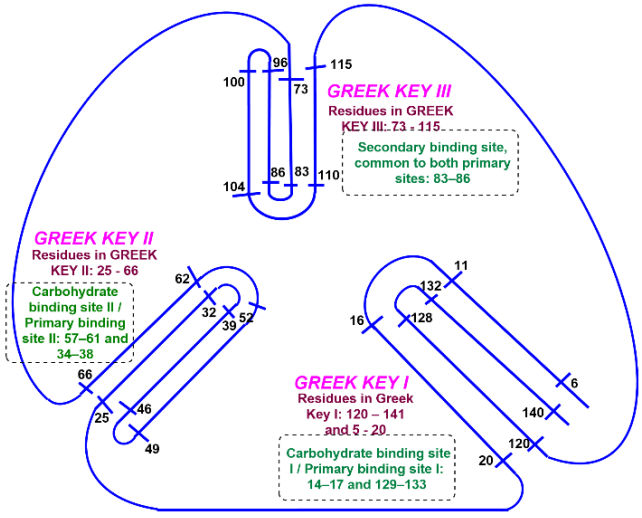

Scheme 1: Schematic illustration of the structural topology of Banlec, illustrating its β-prism I fold, Greek key motifs, and reported carbohydrate-binding sites.

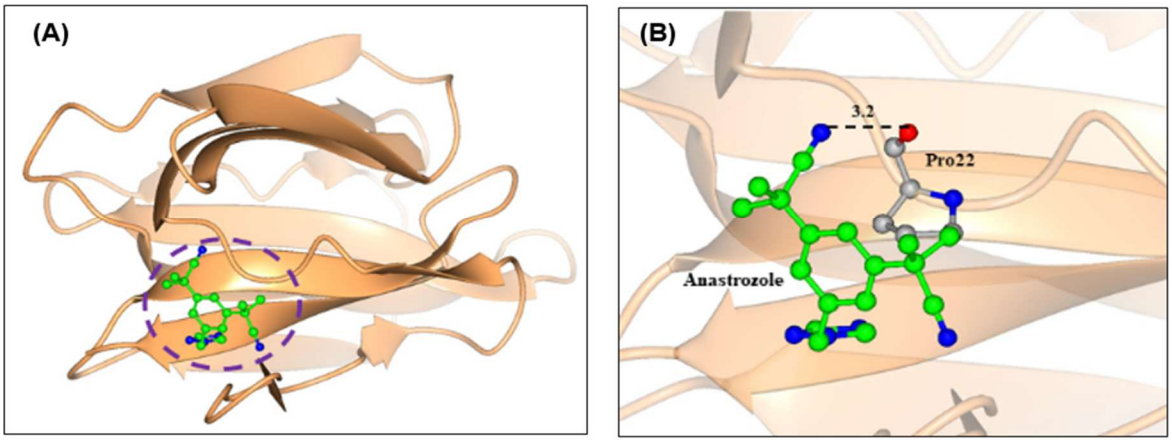

Fig. 6: Molecular docking studies of anastrozole with Banlec. (A) Overall binding orientation of anastrozole on the Banlec surface, (B) Three-dimensional docking pose highlighting the key interacting residues of Banlec involved in stabilizing the anastrozole complex.

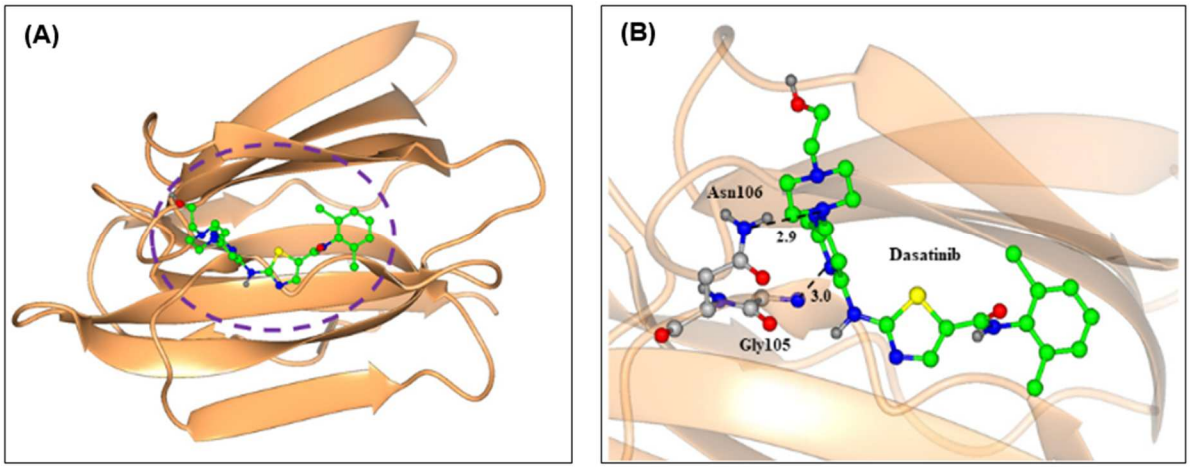

Fig. 7: Molecular docking studies of dasatinib with Banlec. (A) Overall binding orientation of dasatinib on the Banlec surface, (B) Three-dimensional docking pose highlighting the key interacting residues of Banlec involved in stabilizing the dasatinib complex.

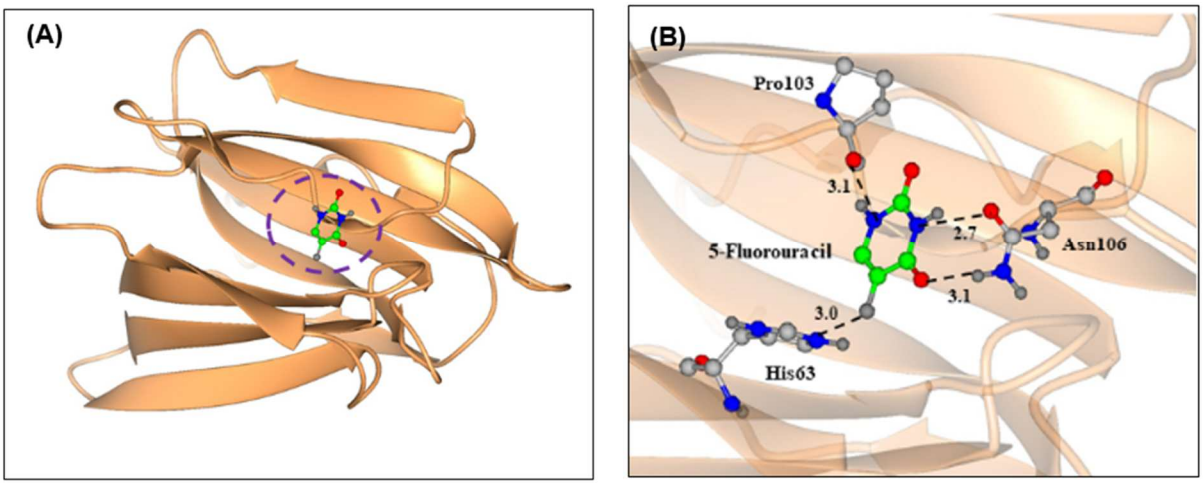

Fig. 8: Molecular docking studies of 5-FU with Banlec. (A) Overall binding orientation of 5-FU on the Banlec surface, (B) Three-dimensional docking pose highlighting the key interacting residues of Banlec involved in stabilizing the 5-FU complex.

Overall, the RMSD results show that dasatinib (C1) serves the most to stabilize the Banlec structure, while anastrozole (C3) leads to relatively greater conformational dynamics during the simulation period.

RMSF analysis was performed to examine residue-level flexibility over ligand binding (Fig. 10). RMSF analyses revealed that the overall fluctuations of the protein framework in the simulated systems remained relatively small across most residues, showing a stable structural conformation across the simulation period. The comparison analysis showed that ligand binding slightly influenced the dynamic behavior of the protein, especially at specific loop regions. In particular, distinct fluctuation peaks were observed between residues 45-50, 65-70, 80-85 and 110-120, implying these regions undergo increased mobility and may contribute to conformational adaptability upon ligand interaction. Among the studied systems, the ligand-bound complexes displayed fluctuating patterns roughly comparable to the *apo* state. However, the Banlec-anastrozole (C3) complex showed comparatively higher fluctuations, especially around residues 50-135, suggesting relatively weaker stabilization or greater conformational flexibility compared to Banlec–dasatinib (C1) and Banlec–5-FU (C2) complexes.

The radius of gyration (RoG) was analyzed to better understand the compactness and folding stability of the *apo* protein and its ligand-bound complexes during the 100 ns MD simulation. All systems displayed stable RoG values with slight fluctuations observed, showing maintenance of a compact protein structure across the simulation, as shown in Fig. 11. The *apo* protein remains steady around 1.42-1.44 nm, whereas the complexes with dasatinib (C1), 5-fluorouracil (C2) and anastrozole (C3) display comparable RoG patterns. Despite slight variations observed in the ligand-bound systems, particularly in the Banlec–5-FU (C2) and Banlec-anastrozole (C3) complexes, especially at later time points, the changes were minimal and remained within a narrow range. However, Banlec-anastrozole (C3) complex exhibited a subtle but consistent upward shift and broader fluctuations, implying slightly reduced structural compactness relative to Banlec–dasatinib (C1) and Banlec–5-FU (C2), though the differences remained small.

Anticancer activity against human leukemic HL-60 cells

The anticancer potential of Banlec and its drug-bound complexes was evaluated against HL-60 (human acute promyelocytic leukemia) cells using the MTT assay. Results revealed that the tested samples exhibited antiproliferative potentials on HL-60 cells to varying degrees. Banlec alone exhibited antiproliferative activity with an IC_{50} value of 0.1324 ± 0.0021 mg/mL (Table 2). 5-FU showed notable anticancer activity with an IC_{50} value of 0.0139 ± 0.0007 mg/mL. However, when Banlec was complexed with 5-FU, a remarkable enhancement in anticancer activity was observed. The IC_{50} value of the Banlec–5-FU complex (0.0003 ± 0.0000578 mg/mL) was substantially lower than both 5-FU alone (0.0139 ± 0.0007 mg/mL) and Banlec alone (0.1324 ± 0.0021 mg/mL) (Table 2). The marked reduction in IC_{50} for the Banlec–5-FU complex suggested a synergistic effect.

In contrast, anastrozole (IC_{50} = 0.00736 ± 0.00013 mg/mL) and dasatinib (IC_{50} = 0.0126 ± 0.000033 mg/mL) exhibited potent anticancer activity in their free forms; however, upon complexation with Banlec, decreased anticancer activity was observed, as evidenced by higher IC_{50} values (0.1232 ± 0.0022 mg/mL and 0.1987 ± 0.0020 mg/mL, respectively) (Table 2). These findings indicate that the modulatory effect of Banlec is drug-dependent, enhancing the anticancer activity of 5-FU while reducing the efficacy of anastrozole and dasatinib under the tested conditions

DISCUSSION

In the present study, Banlec was purified from ripened banana fruit, and its binding interactions with anticancer drugs (i.e., anastrozole, dasatinib and 5-FU) were examined using spectroscopic and computational techniques, as well as biological assays. The initial UV–Visible spectroscopic analyses provide crucial insight into the formation of stable Banlec–drug complexes. Based on both binding constant (K_b) and Gibbs free energy ($\Delta G°$) values, the overall binding affinity followed the order; Banlec-dasatinib > Banlec-5-FU > Banlec-anastrozole, with dasatinib forming the most stable and spontaneous complex ($\Delta G°$ = -29.7 kJ mol^{-1}). These findings highlight the significance of this first step in elucidating the binding between Banlec and anticancer drugs, providing a foundation for deeper structural and functional characterization in subsequent studies.

Circular dichroism (CD) spectroscopic analyses indicated that Banlec preserved its secondary structure upon interaction with dasatinib and 5-FU. Differential scanning fluorimetry (DSF) results revealed that the Banlec-dasatinib and Banlec-5-FU complexes showed a stabilizing effect on the protein structure, whereas the Banlec-anastrozole complex suggested a destabilizing effect. Hemagglutination inhibition assay results further indicated that drug binding did not mask the Banlec's carbohydrate-binding domains, preserving its hemagglutination activity; hence, the targeting potential of the proposed vehicle (i.e., Banlec) is not lost.

In silico studies (i.e., molecular docking and simulations) further help to explore the binding interactions of Banlec with selected anticancer drugs. It is well reported that Banlec exists as a homodimer, with each subunit having a molecular weight of approximately 15 kDa. Each monomer adopts a β-prism I fold composed of 12 β-strands arranged into three four-stranded Greek key motifs (I–III).

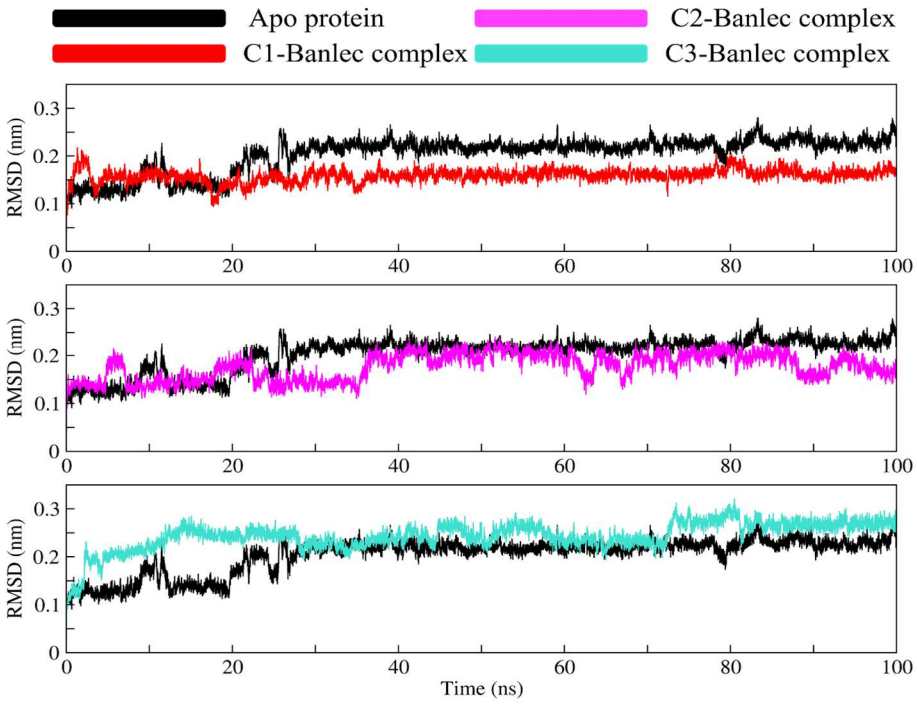

Fig. 9: RMSD plots showing the structural stability of the *apo* protein and its complexes with three drugs, Dasatinib (C1), 5-Fluorouracil (C2), and Anastrozole (C3), over a 100 ns of molecular dynamics simulation.

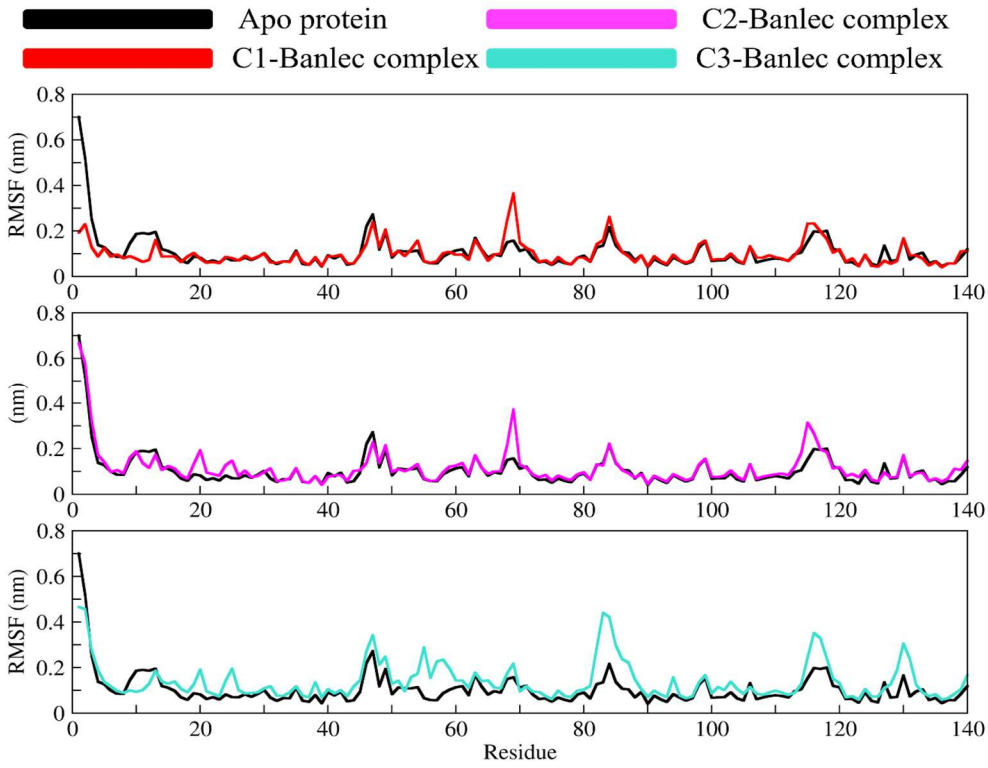

Fig. 10: RMSF plots illustrating the residue-wise flexibility and structural stability of the *apo* protein and its complexes with three drugs, Dasatinib (C1), 5-Fluorouracil (C2), and Anastrozole (C3), over a 100 ns molecular dynamics simulation.

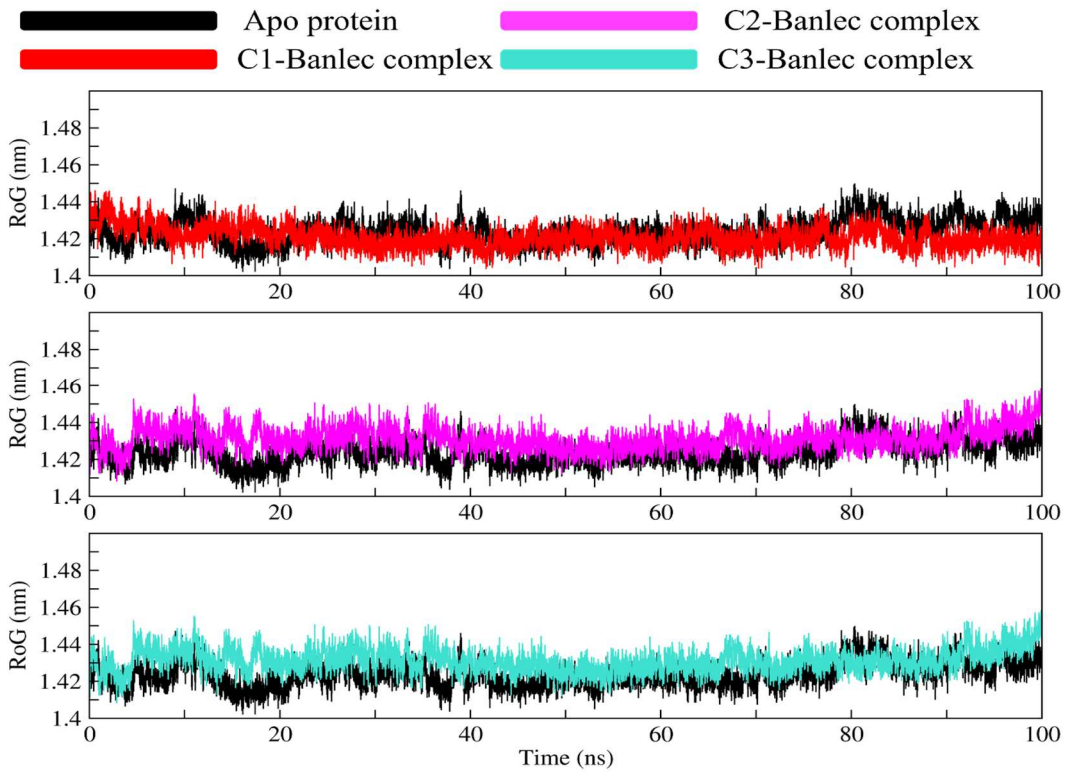

Fig 11: Radius of gyration (RoG) plots representing the structural compactness of the *apo* protein and its complexes with Dasatinib (C1), 5-Fluorouracil (C2), and Anastrozole (C3) over a 100 ns molecular dynamics simulation.

Table 2: Anticancer activities of Banlec and its complexes evaluated against HL-60 cell line.

S. No.	Complex	IC_{50} ± SEM (mg/mL)
1.	Banlec	0.1324 ± 0.0021
2.	5-Fluorouracil	0.0139 ± 0.0007
3.	Banlec-5-Fluorouracil complex	0.0003 ± 0.0000578
4.	Anastrozole	0.00736 ± 0.00013
5.	Banlec-Anastrozole complex	0.1232 ± 0.0022
6.	Dasatinib	0.0126 ± 0.000033
7.	Banlec- Dasatinib complex	0.1987 ± 0.0020

Banlec possesses two primary carbohydrate-binding sites: CBS I (residues 14–17 and 129–133) located on Greek key I and CBS II (residues 34–38 and 57–61) situated on Greek key II. A secondary binding site, common to both CBSs, has also been reported within residues 83–86 of Greek key III. (Scheme-1) (Singh *et al.*, 2005; Meagher *et al*., 2005). Given this structural organization and the presence of well-defined sugar-binding pockets, blind docking was performed to examine the potential interactions between Banlec and the selected anticancer drugs, and to determine whether these ligands preferentially bind at the carbohydrate recognition sites or at alternative allosteric regions on the protein surface. The results of molecular docking showed strongest binding with dasatinib, providing maximal stabilization, followed by 5-FU with moderate stabilization. These results demonstrate that Banlec is capable of accommodating structurally diverse anticancer compounds through specific hydrogen-bonding interactions at both carbohydrate-binding and alternative allosteric sites. The observed binding affinities and interaction profiles highlight the versatility of Banlec, suggesting its potential utility in drug delivery. Molecular dynamics simulation further supported the docking results, confirming the stability of Banlec–drug complexes over time. The MD simulations showed that Banlec maintained overall structural stability in both *apo* and ligand-bound forms. Among the selected ligands, dasatinib was found to effectively stabilize the protein, while anastrozole induced greater flexibility and conformational fluctuations. The anticancer activity results indicate that Banlec modulates the efficacy of the selected drugs in a ligand-dependent manner. Complexation with 5-FU markedly enhanced antiproliferative activity, showing greater efficacy than 5-FU alone, indicating a synergistic effect. In contrast,

Banlec-anastrozole and Banlec-dasatinib complexes showed reduced activity compared to the free drugs, highlighting the selective modulatory role of Banlec. Overall, the combined spectroscopic, computational, and biological analyses provide insight into Banlec's structural stability, ligand interactions, and modulatory potential.

CONCLUSION

In conclusion, this study systematically investigated the isolation and purification of Banlec as a ~30 kDa homodimeric protein, as well as its binding interactions with three selected FDA-approved anticancer drugs. The interactions were evaluated using UV–Visible spectroscopy, circular dichroism (CD) spectroscopy, differential scanning fluorimetry (DSF), molecular docking, molecular dynamics simulation studies, and further supported by cell-based studies against HL-60 cells using the MTT assay. Binding analyses revealed that dasatinib exhibited the strongest affinity toward Banlec ($K_b = (1.65 \pm 0.09) \times 10^5\ M^{-1}$), followed by 5-FU ($K_b = (1.41 \pm 0.03) \times 10^5\ M^{-1}$), while anastrozole showed a weaker interaction ($K_b = (5.1 \pm 0.03) \times 10^2\ M^{-1}$). CD and DSF studies indicated that dasatinib and 5-FU stabilized Banlec's structure (ΔTm = +0.8°C and +1.4°C, respectively), whereas anastrozole induced structural destabilization (ΔTm = -1.7°C), indicating its limited compatibility with Banlec as a drug-delivery scaffold. Hemagglutination inhibition assays confirmed that the selected drugs did not interfere with Banlec's carbohydrate-binding activity, indicating that its lectin function is preserved. Molecular docking studies supported these observations, highlighting specific hydrogen-bonding interactions of dasatinib with Gly105 and Asn106, 5-FU with Pro103, Asn106 and His63 and anastrozole primarily with Pro22. Molecular dynamics simulations further validated these findings at an atomic level, revealing ligand-dependent effects on Banlec's structural stability, flexibility and compactness. Dasatinib most effectively stabilized the Banlec, followed by 5-FU, while anastrozole induced higher conformational fluctuations and flexibility. Additionally, among the three analyzed complexes, the Banlec–5-FU complex exhibited the most pronounced anticancer activity against the HL-60 cells, with efficacy significantly higher than that of both Banlec alone and 5-FU alone. Collectively, these results demonstrate Banlec's capacity to accommodate structurally diverse anticancer drugs, supporting its versatility and potential biological relevance and hence may have potential for further investigation in glycan-related applications. However, these observations are preliminary and further studies are required to validate complex stability and functionality in *in vivo* models to better understand the translational potential of Banlec-based drug delivery systems in cancer therapy. Future investigations will therefore focus on evaluating the stability and behavior of the most promising complex, particularly Banlec–5-FU, under physiologically relevant conditions, including serum stability assays, competitive binding with plasma proteins and carbohydrates and time-dependent monitoring of structural integrity.

Acknowledgements
Not applicable

Authors' contributions
Rida Arif: Methodology, investigation, visualization, writing-original draft.
Javeria Arif: Methodology, visualization, writing-review and editing.
Zoha Warsi, Methodology, visualization.
Syeda Sarah Tahir, Methodology, visualization.
Saima Rasheed: Conceptualization, methodology, software, validation, formal analysis, investigation, resources, data curation, writing-original draft preparation, writing-review and editing, visualization, supervision, project administration, funding acquisition.

Funding
There was no funding.

Data availability statement
All data generated or analysed during this study are included in this article.

Ethical approval
The experimental protocol was approved by the "Independent Ethics Committee (IEC)" of the ICCBS, University of Karachi under Study #ICCBS/IEC-098-HB/2023 and written informed consent was taken from participants prior to sample collection.

Conflict of interest
There are no conflicts of interest to declare.

REFERENCES

Abdi K, Nafisi SH, Manouchehri F, Bonsaii M and Khalaj A (2012). Interaction of 5-fluorouracil and its derivatives with bovine serum albumin. *J. Photochem. Photobiol. B.,* **107**: 20-26.

Abraham MJ, Murtola T, Schulz R, Pall S, Smith JC, Hess B and Lindahl E (2015). GROMACS: High performance molecular simulations through multi-level parallelism from laptops to supercomputers. *SoftwareX*, **1**: 19-25.

Adamova L, Malinovska L and Wimmerova M (2014). New sensitive detection method for lectin hemagglutination using microscopy. *Microsc. Res. Tech.,* **77**(10): 841-849.

Adamczyk O, Szota M, Rakowski K, Prochownik M, Doveiko D, Chen Y and Jachimska B (2023). Bovine serum albumin as a platform for designing biologically active nanocarriers—experimental and computational studies. *Int. J. Mol. Sci.,* **25**: 37.

Azeem K, Abdulhameed HT, Hussain A, Amir S, Parveen M, Patel R and Abid M (2024). A comprehensive multispectroscopic and computational analysis of the interaction between plant-based antiplasmodial compounds and bovine serum albumin. *ACS Omega*, **9**(5): 5576-5591.

Batcha ATM, Wadhwani A and Subramaniam G (2020). *In vitro* antiviral activity of BanLec against herpes simplex viruses type 1 and 2. *Bangladesh J. Pharmacol*., **15**(1): 11-18.

Boliukh I, Rombel-Bryzek A and Bułdak RJ (2024). Lectins in oncology and virology: Mechanisms of anticancer activity and SARS-CoV-2 inhibition. *Int. J. Biol. Macromol.,* **275**: 133664.

Chitongo R, Obasa AE, Mikasi SG, Jacobs GB and Cloete R (2020). Molecular dynamic simulations to investigate the structural impact of known drug resistance mutations on HIV-1C integrase-dolutegravir binding. *PLoS One*, **15**(5): e0223464.

Cheung AH, Wong JH and Ng TB (2009). *Musa acuminata* (Del Monte banana) lectin is a fructose-binding lectin with cytokine-inducing activity. *Phytomedicine*, **16**(6-7): 594-600.

De Camargo LJ, Picoli T, Fischer G, de Freitas ACO, de Almeida RB and da Silva Pinto L (2020). Antiviral activity of native banana lectin against bovine viral diarrhea virus and bovine alphaherpesvirus type 1. *Int. J. Biol. Macromol.,* **157**: 569-576.

Degroote RL, Korbonits L, Stetter F, Kleinwort KJ, Schilloks MC, Amann B, Hirmer S, Hauck SM and Deeg CA (2021). Banana lectin from *Musa paradisiaca* is mitogenic for cow and pig PBMC via IL-2 pathway and ELF1. *Immuno*, **1**(3): 264-276.

Gnanesh Kumar BS and Surolia A (2018). Identification of banana lectin isoforms and differential acetylation through mass spectrometry approaches. *Protein J*., **37**: 38-46.

Gupta G, Sinha S and Surolia A (2008). Unfolding energetics and stability of banana lectin. *Proteins*, **72**(2): 754-760.

Hornak V, Abel R, Okur A, Strockbine B, Roitberg A and Simmerling C (2006). Comparison of multiple Amber force fields and development of improved protein backbone parameters. *Proteins: Struct. Funct. Bioinform.,* **65**(3): 712-725.

Jorgensen WL, Chandrasekhar J, Madura JD, Impey RW and Klein ML (1983). Comparison of simple potential functions for simulating liquid water. *J. Chem. Phys.,* **79**(2): 926-935.

Khan JM, Qadeer A, Ahmad E, Ashraf R, Bhushan B, Chaturvedi SK, Rabbani G and Khan RH (2013). Monomeric banana lectin at acidic pH overrules conformational stability of its native dimeric form. *PLoS One*, **8**(4): 62428.

Koshte VL, Van Dijk W, Van Der Stelt ME and Aalberse RC (1990). Isolation and characterization of BanLec-I, a mannoside-binding lectin from *Musa paradisiaca* (banana). *Biochem. J.*, **272**(3): 721-726.

Lavelle EC, Grant G, Pfuller U and O'Hagan DT (2004). Immunological implications of the use of plant lectins for drug and vaccine targeting to the gastrointestinal tract. *J. Drug Target.*, **12**(2): 89-95.

Liu XY, Li H and Zhang W (2014). The lectin from *Musa paradisiaca* binds with the capsid protein of tobacco mosaic virus and prevents viral infection. *Biotechnol. Biotechnol. Equip.*, **28**(3): 408-416.

Mahaboob Batcha ATM, Subramaniam G and Venkatachalam K (2023). Purified Banana lectin (BanLec) isolated from the ripen pulp of *Musa Paradisiaca* induces apoptosis in cancer cell lines: *In vitro* study. *ADTM.*, **23**(2): 589-604.

Martonak R, Laio A and Parrinello M (2003). Predicting crystal structures: The Parrinello-Rahman method revisited. *Phys. Rev. Lett.,* **90**(7): 075503.

Martyna GJ, Klein ML and Tuckerman M (1992). Nose–Hoover chains: The canonical ensemble *via* continuous dynamics. *J. Chem. Phys.,* **97**(4): 2635-2643.

McNicholas S, Potterton E, Wilson KS and Noble MEM (2011). Presenting your structures: The CCP4mg molecular-graphics software. *Acta Crystallogr. D Biol. Crystallogr.*, **67**(4): 386-394.

Meagher JL, Winter HC, Ezell P, Goldstein IJ and Stuckey JA (2005). Crystal structure of banana lectin reveals a novel second sugar binding site. *Glycobiology,* **15**(10): 1033-1042.

Micsonai A, Wien F, Kernya L, Lee YH, Goto Y, Refregiers M and Kardos J (2015). Accurate secondary structure prediction and fold recognition for circular dichroism spectroscopy. *Proc. Natl. Acad. Sci. U.S.A.*, **112**(24): 3095-3103.

Morris GM, Huey R and Olson AJ (2008). Using AutoDock for ligand-receptor docking. *Curr. Protoc. Bioinform.*, **24**(1): 8-14.

Munir I, Ajmal S, Shah MR, Ahmad A, Hameed A and Ali SA (2017). Protein-drug nanoconjugates: Finding the alternative proteins as drug carrier. *Int. J. Biol. Macromol.*, **101**: 131-145.

Nazir F, Munir I and Yesiloz G (2024). A microfluidics-assisted double-barreled nanobioconjugate synthesis introducing aprotinin as a new moonlight nanocarrier protein: Tested toward physiologically relevant 3D-spheroid models. *ACS Appl. Mater. Interfaces*, **16**(15): 18311-18326.

Naithani S, Komath SS, Nonomura A and Govindjee G (2021). Plant lectins and their many roles: Carbohydrate-binding and beyond. *J. Plant Physiol.,* **266**: 153531.

Neetu, Ahlawat S, Delipan R, Ringe RP, Rao A and Ramya TNC (2025). Identification of SARS-CoV-2-binding lectins on a commercial lectin array. *Sci. Rep.,* **15**(1): 21687.

Peumans WJ, Zhang W, Barre A, Houles Astoul C, Balint-Kurti PJ, Rovira P, Rouge P, May GD, Van Leuven F,

Truffa-Bachi P and Van Damme EJ (2000). Fruit-specific lectins from banana and plantain. *Planta*, **211**(4): 546-554.

Rahman A, Noor F, Ashfaq UA, Darwish HW, Aschner M, Din ZU and Khan H (2024). Multitarget mechanisms of monocarbonyl curcuminoid analogues against HL-60 cancer cells: *In vitro* and network pharmacology-based approach. *ACS Omega,* **9**(10): 11836-11847.

Santos VF, Costa MS, Campina FF, Rodrigues RR, Santos AL, Pereira FM, Batista KL, Silva RC, Pereira RO, Rocha BA and Coutinho HD (2020). The galactose-binding lectin isolated from Vatairea macrocarpa seeds enhances the effect of antibiotics against *Staphylococcus aureus*–resistant strain. *Probiotics Antimicro. Proteins*, **12**(1): 82-90.

Singh DD, Saikrishnan K, Kumar P, Dauter Z, Sekar K, Surolia A and Vijayan M (2004). Purification, crystallization and preliminary X-ray structure analysis of the banana lectin from *Musa paradisiaca*. *Acta Crystallogr. D Biol. Crystallogr.*, **60**(11): 2104-2106.

Singh DD, Saikrishnan K, Kumar P, Surolia A, Sekar K and Vijayan M (2005). Unusual sugar specificity of banana lectin from *Musa paradisiaca* and its probable evolutionary origin. Crystallographic and modelling studies. *Glycobiology*, **15**(10): 1025-1032.

Singh SS, Devi SK and Ng TB (2014). Banana lectin: A brief review. *Molecules*, **19**(11): 18817-18827.

Sousa da Silva AW and Vranken WF (2012). ACPYPE–Antechamber python parser interface. *BMC Res. Notes.,* **5**(1): 367.

Swanson MD, Winter HC, Goldstein IJ and Markovitz DM (2010). A lectin isolated from bananas is a potent inhibitor of HIV replication. *J. Biol. Chem.*, **285**(12): 8646-8655.

Wong JH and Ng TB (2006). Isolation and characterization of a glucose/mannose-specific lectin with stimulatory effect on nitric oxide production by macrophages from the emperor banana. *Int. J. Biochem. Cell Biol.*, **38**(2): 234-243.

Yin Y, Chen D, Qiao M, Lu Z and Hu H (2006). Preparation and evaluation of lectin-conjugated PLGA nanoparticles for oral delivery of thymopentin. *J. Control Release*, **116**(3): 337-345.

Zhou J, Hao N, De Zoyza T, Yan M and Ramstrom O (2015). Lectin-gated, mesoporous, photo functionalized glyconanoparticles for glutathione-responsive drug delivery. *Chem. Commun. (Camb).*, **51**(48): 9833-9836.

Zhu S, Yang S, Chen Y, Niu MM, Wang J, Li J and Pu X (2025). Identification of a novel and high affinity MIF inhibitor *via* structure-based pharmacophore modelling, molecular docking, molecular dynamics simulations and biological evaluation. *J. Enzyme Inhib. Med. Chem.,* **40**(1): 2501378.